

Properties of ferromagnetic film hysteresis, on the surface of a hard-magnetic antiferromagnet, with a domain structure

Cite as: Low Temp. Phys. **40**, 990 (2014); <https://doi.org/10.1063/1.4901921>

Published Online: 03 December 2014

A. S. Kovalev, and M. L. Pankratova



View Online



Export Citation



CrossMark

ARTICLES YOU MAY BE INTERESTED IN

[The magnetic structure of a thin ferromagnetic film on the rough surface of an antiferromagnet](#)
Low Temperature Physics **37**, 866 (2011); <https://doi.org/10.1063/1.3671860>



LOW TEMPERATURE TECHNIQUES
OPTICAL CAVITY PHYSICS
MITIGATING THERMAL
& VIBRATIONAL NOISE

DOWNLOAD THE WHITE PAPER

downloads.montanainstruments.com/optical_cavities

MONTANA INSTRUMENTS
COLD SCIENCE MADE SIMPLE

Properties of ferromagnetic film hysteresis, on the surface of a hard-magnetic antiferromagnet, with a domain structure

A. S. Kovalev

B. Verkin Institute of Low Temperature Physics and Engineering of the National Academy of Sciences of Ukraine, 47 Lenin Ave., Kharkov 61103, Ukraine and V. N. Karazin Kharkov National University, 4 Svoboda Sq., Kharkov 61077, Ukraine

M. L. Pankratova^{a)}

B. Verkin Institute of Low Temperature Physics and Engineering of the National Academy of Sciences of Ukraine, 47 Lenin Ave., Kharkov 61103, Ukraine

(Submitted July 4, 2014)

Fiz. Nizk. Temp. **40**, 1267–1280 (November 2014)

This is a theoretical investigation of the exchange bias phenomenon, and the properties of a thin magnetic film's magnetization hysteresis loop, on the rough surface of a hard-magnetic antiferromagnet. An interface model with a periodic structure of atomic steps is presented. These atomic steps are associated with a spatially inhomogeneous distribution of the ferromagnetic film magnetization, akin to a system of domain walls. This structure leads to a complicated external field dependence of magnetization: the hysteresis curve can assume an asymmetrical shape and “fall apart” into two hysteresis loops, divided by a “horizontal plateau,” or an area with constant field-independent magnetization. Such field dependence behavior has been recently observed experimentally in different ferro/antiferromagnet systems. The field dependence of magnetization has been obtained analytically using the long-wave approximation for various characteristics of ferromagnetic film (its thickness, values of exchange interaction, and magnetic anisotropy), and the interface (the period of the inhomogeneous structure, and exchange interaction through the interface). The analytical results are confirmed by numerical calculations for the corresponding discrete model with a more complex interface structure. © 2014 AIP Publishing LLC.

[<http://dx.doi.org/10.1063/1.4901921>]

1. Introduction

Recently, due to the technological applications of multi-layer magnetic systems,^{1,2} there have been intense experimental and theoretical investigations of the magnetic properties of contacting ferro- (FM) and antiferromagnetic (AFM) thin film. A long time ago,³ it was discovered that during such contact, there is a shift in the field dependence of magnetization, $M = M(H)$ from the symmetrical position, relative to the field magnitude (*exchange bias*, (EB)). The simplest explanation for this effect is as follows: a hard-magnetic AFM (or FM) with a fixed direction of magnetic moments and an “uncompensated” surface (nonzero average magnetization of the surface atomic layer) creates a local field that is independent of the external field, at the interface of the thin FM film, with which it has contact. This model provides a quality description of a shift in the field dependence hysteresis loop, in the case of an ideal interface between the FM/ layered AFM, with the layers parallel to the interface itself.^{2,4–8} However, the EB is observed even in the case of a compensated boundary, and can be explained by non-ideality (roughness) of the interface. The latest experiments have shown^{9–11} that aside from EB, the field dependence of magnetization can have additional, and fairly complex properties: the appearance of a “horizontal plateau” with constant magnetization in a range of fields, the differing of the slope of the $M = M(H)$ dependence, in accordance to different field values, and the hysteresis loop itself “splitting” into two symmetrical or asymmetrical loops.

With an ideal interface, this behavior can be explained by inhomogeneous FM film magnetization, similar to domain walls (DW), parallel to the interface. Another possibility is related to the interface roughness, resulting in the spatial inhomogeneity of the magnetization in the contact plane, resembling DW, but with a perpendicular orientation to the interface.^{12–14} In this case, the EB phenomenon and nonstandard $M = M(H)$ dependence, can be examined independently (even though their origins are the same, i.e., AFM influence on the FM film). If the average magnetization of the surface AFM layer is $\langle M_s \rangle = 0$, then EB is absent, but the sloped portions of the field dependence, horizontal plateau, and the split hysteresis loops, could remain.^{15,16} All indicated phenomena essentially depend on the nature of the interface roughness. In some cases magnetic contact through the interface exists only for a small number of surface FM and AFM atoms (magnetic point contacts).¹⁷ In other cases, lines of atomic steps (AS) can form at the AFM surface, dividing the AFM surface regions with oppositely directed magnetic moments.^{13,14} If the surface is, on average, homogeneous, then the interface has alternating steps with opposite signs. A one-dimensional model of such a system was presented by us in Ref. 14, where we demonstrated that DW are connected to the presence of such steps at the interface, which divide the FM film into domains with different magnetization orientation. In this case the film was considered to be sufficiently thick to cause DW bending within the film.

This study examines a one-dimensional model of FM/AFM contact with periodically distributed atomic steps at

the interface, in the case of a thin FM film, for which changes in the FM magnetization volume can be neglected. If surface regions with opposite magnetization direction at the subsurface AFM layer have identical values, then in this model there is no EB, but other characteristic properties of the $M=M(H)$ dependence observed in experiments, can remain. When widths are alternated for different interface sections, there is a manifestation of EB, and field dependence becomes asymmetrical. An extreme case of a big difference in the size of the regions with opposing magnetization, corresponds to the model examined earlier in Ref. 17.

2. Model formulation

A diagram of the examined model is presented in Fig. 1. Plane-parallel monoatomic step defects with alternating signs are located at the interface. The period of the L structure is assumed to be much longer than then interatomic distance a , which allows us to consider the problem using the long-wave approximation. In the simplest case $b=L/2$, the average magnetization of the subsurface AFM layer is equal to zero, and EB is absent. If $b \neq L/2$, the interface structure is doubly periodic, the average magnetization at the AFM surface is other than zero, and there is EB. The AFM magnetic moments are fixed (hard-magnetic AFM), whereas FM moments change their orientation in the external magnetic field. The step defects form bands, in which magnetization of the subsurface AFM layer runs in an anti-parallel direction. In addition, this model can describe systems with an ideal interface, in which bands of domains formed in the AFM part of the subsystem, after demagnetization by an alternating field with a decreasing amplitude at a temperature below the Curie point, but above the blocking point.^{15,16} The FM film contains a small number of n layers, and the change in the magnetization across its thickness is neglected. For the purpose of simplification, we assume that the ferromagnet has a strong magnetic anisotropy akin to an “easy plane” (caused, for example, by the magnetic dipole interaction) and that the magnetic moments are located, and can rotate, within this plane. In addition, there is the possibility of the existence of an additional weak magnetic anisotropy in the easy plane, the axis of which (easy axis) corresponds to the orientation of the AFM magnetic moments. The direction of the external magnetic field is also expected to coincide with it.

The proposed simple model is described by the scalar equation for the angles of magnetization rotation in the easy plane $\varphi(x)$, calculated from this derived direction. The X axis is chosen in the interface plane as the direction of the periodic structure of the atomic steps.

The energy of the FM system can be written as

$$E = \frac{M_0^2}{a} \int dx \left(\frac{Jn}{2} a^2 (\varphi')^2 - \tilde{J}_0 f(x) \cos \varphi - \frac{\beta n}{2} \cos^2 \varphi - H n \cos \varphi \right), \quad (1)$$

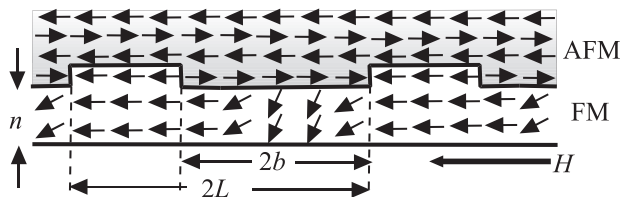


FIG. 1. A model of the rough stepped AFM/FM film border.

where J is the FM exchange interaction constant, β is the magnetic anisotropy constant in the easy plane, \tilde{J}_0 is the FM and AFM exchange interaction through the interface, M_0 is the nominal magnetization, and a prime stands for the derivative with respect to X . Assuming the interface to be even, we model its stepped features in the special case of $b=L/2$, introducing the function

$$f = 2 \sum_{s=-\infty}^{\infty} \left[\theta \left(x - \frac{4s-1}{2} L \right) - \theta \left(x - \frac{4s+1}{2} L \right) \right] - 1, \quad (2)$$

provided in Fig. 2, where $\theta(x)$ is the Heaviside function, and s stands for the natural numbers.

It is convenient to renormalize the total energy using the effective exchange interaction through the interface $J_0 = \tilde{J}_0/n$, taking into account further on, that at a low FM film thickness, this interaction is several times smaller than the real exchange through the interface.

Equations describing the distribution of FM magnetization, have the following form:

$$-Ja^2 \varphi_A'' + (H + J_0) \sin \varphi_A + \beta \sin \varphi_A \cos \varphi_A = 0 \quad \text{in regions A,} \quad (3)$$

$$-Ja^2 \varphi_B'' + (H - J_0) \sin \varphi_B + \beta \sin \varphi_B \cos \varphi_B = 0 \quad \text{in regions B,} \quad (4)$$

where the regions A and B are marked in Fig. 2. Formally, they coincide with equations that describe the non-linear parametric resonance in mechanics. Equations (3) and (4) must be supplemented by boundary conditions, which take into consideration the lattice discreteness along the X axis, at the locations of the atomic steps on the surface. In large external fields, the magnetization is directed along the field in these major states $\varphi = 0$ ($\mathbf{H} \parallel \mathbf{n}_x$) or $\varphi = \pi$ ($\mathbf{H} \parallel -\mathbf{n}_x$). At critical fields $H = \pm H_0$ the FM film transitions to a spatially inhomogeneous state with $\varphi = \varphi(x)$. In the proximity of the critical fields, the turn of the $\varphi(x)$ angle is smooth, and the long-wave approximation boundary conditions for (3) and (4) at the interface steps (at the points where $x = x_s = (1 + 2s)b$, $b = L/2$) look like

$$\varphi_A|_s = \varphi_B|_s, \quad \varphi_A'|_s = \varphi_B'|_s. \quad (5)$$

Aside from the indicated homogeneous conditions, the examined system allows for inhomogeneous anti-collinear

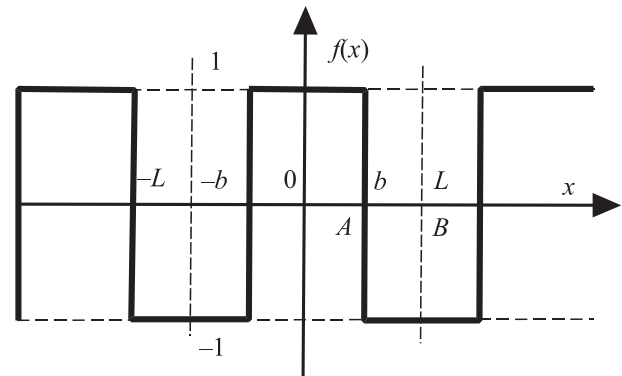


FIG. 2. Profile of the exchange interaction through the FM/AFM border, for a compensated interface ($b = L/2$).

states, in which, for domains A and B , the magnetization is oriented strictly with and against the field: for example, for one field orientation $\varphi_A = 0$ and $\varphi_B = \pi$. In this state, the total magnetization is equal to zero for a certain interval of the field, symmetric with respect to its sign. Here, at the interface steps, the φ angle changes by a jump. At these points, the long-wave approximation cannot be justified, and it is necessary to consider the discreteness of the system. If within the A and B domains themselves, it is possible to stay within the framework of the long-wave Eqs. (3) and (4), which is justified by a large magnetic length $l_0 = \sqrt{J/\beta a} \gg a$, then the boundary conditions must be upgraded. When taking into consideration the discreteness of the system, the first term in (1) is substituted by the expression $-Jn\cos(\varphi_i - \varphi_{i-1})$, where the index i numbers atoms in the direction of the X axis. In Eqs. (3) and (4) the first terms are rewritten in the form $J\sin(\varphi_i - \varphi_{i-1}) - J\sin(\varphi_i - \varphi_{i+1})$. These circumstances result in the following boundary conditions:

$$a\varphi'_A|_s = \sin(\varphi_B - \varphi_A)|_s, \quad a\varphi'_B|_s = \sin(\varphi_B - \varphi_A)|_s, \quad (6)$$

from which we can derive that $\varphi'_A|_s = \varphi'_B|_s$. In the long-wave approximation $a(d/dx) \ll 1$, and from (6) we get the condition (5) $\varphi_A|_s = \varphi_B|_s$. However, for states close to anti-collinear, it is necessary to use expression (6). Using simpler boundary conditions from (5) makes strictly anti-collinear states disappear, and regions of field dependence with $M = \text{const}$ turn into regions with a weak dependence of magnetization on the field. Since the main objective is to calculate the experimentally observed dependence of the magnetization on the external field $M = M(H)$, we present an expression for the magnitude of FM film magnetization along the length of the structure period $\Delta x = 2L$:

$$M = \frac{M_0 n}{a} \left(\int_{-b}^b dx \cos \varphi_A + \int_b^{3b} dx \cos \varphi_B \right). \quad (7)$$

We will start our investigation of possible magnetic structures from a simple FM isotropic limit.

3. Inhomogeneous states of isotropic ferromagnetic film, with a compensated interface ($b = L/2$)

Usually, in the case of an isotropic FM, there is no hysteresis for the magnetization curve, but it can exist in the composite FM/AFM system, and the $M = M(H)$ dependence itself can have a complex character.

First of all, we will find the critical values of the external field $H = \pm H_0$, at which the homogeneous states lose stability, and $H = \pm H_*$, at which the anti-collinear state loses stability with $\varphi_A = 0$, and $\varphi_B = \pi$.

Near the field value $H = H_0$, the linearized Eqs. (3) and (4)

$$Ja^2\varphi''_A - (J_0 + H)\varphi_A = 0, \quad Ja^2\varphi''_B - (J_0 + H)\varphi_B = 0, \quad (8)$$

are solved as

$$\varphi_A = A \text{ch} \left(\sqrt{\frac{J_0 + H}{J}} \frac{x}{a} \right), \quad \varphi_B = B \cos \left(\sqrt{\frac{J_0 + H}{J}} \frac{x - L}{a} \right), \quad (9)$$

which, when substituted into the boundary conditions (5), give the equation for finding the critical field H_0 :

$$P_0 \text{tg}(P_0) = R_0 \text{th}(R_0), \quad (10)$$

where $R_0 = S\sqrt{1 + h_0}$, $P_0 = s\sqrt{1 - h_0}$, $S = \sqrt{J_0/J}(L/2a)$ and $h_0 = H_0/J_0$.

The critical value of the field depends on the parameters of the FM (J), and the interface (J_0 and L). The FM exchange interaction can be considered a given, and the dependence on the parameters of the interface can be conveniently characterized using the values of J_0 and S . (We will note that in the given case of a compensated interface, all system parameters (J, J_0, n, L) are in the form of one combination S). A solution for Eq. (10) in the form of the function $h = h(S)$ is depicted in Fig. 3 by curve H_0 . The asymptotes for large and small values of S look like: $h_0 \approx 1 - (\pi/2S)^2$ at $S \gg 1$ and $h_0 \approx S^2/3$ at $S \ll 1$. A significant change in dependence happens at $S \sim 1$.

Fig. 3, the H_0 curve corresponds to a canted field occurrence, Curves H_* are related fields that limit the “horizontal plateau” of the anti-collinear phase for big and small distances between atomic steps. Values for $L/2a$ are indicated in brackets. The diagram shows that at large values for parameters of S , i.e., at a strong interaction through the interface, or a long period for the dependence structure, $H_0(S)$ and $H_*(S)$ will intersect, such that the hysteresis of the field dependence of magnetization occurs even in the absence of FM magnetic anisotropy. The dependence of $H_0 = H_0(J_0)$ at fixed values of the FM exchange interaction, and the period of the surface structure, is shown in H_0 curves in Fig. 4.

The anti-collinear state exists only when the discreteness of the system is taken into account. Without this, the $M = M(H)$ dependence is unremarkable, and the magnetization decreases monotonically from value $M_m = M_0 2Ln/a$ to $M = -M_m = -M_0 2Ln/a$ when the field changes from H_0 to $-H_0$. The discreteness of the magnet is expressed near the atomic steps at the interface. In the anti-collinear state $\varphi_A = 0$, $\varphi_B = \pi$, total magnetization is absent: $M = 0$. Taking into consideration small deviations of magnetization from this state $\varphi_A \ll 1$, $\varphi_B = \pi - \psi_B$, $\psi_B \ll 1$ and linearizing Eqs. (3) and (4) using these small corrections, we derive the system

$$Ja^2\varphi''_A - (J_0 + H)\varphi_A = 0, \quad Ja^2\psi''_B - (J_0 - H)\psi_B = 0. \quad (11)$$

Solutions for these equations look like

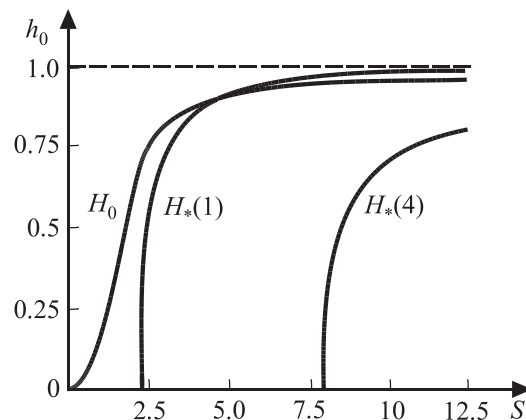


FIG. 3. The dependence of the critical fields on the system parameters L, J, J_0 ($S = \sqrt{J_0/J}(L/2a)$).

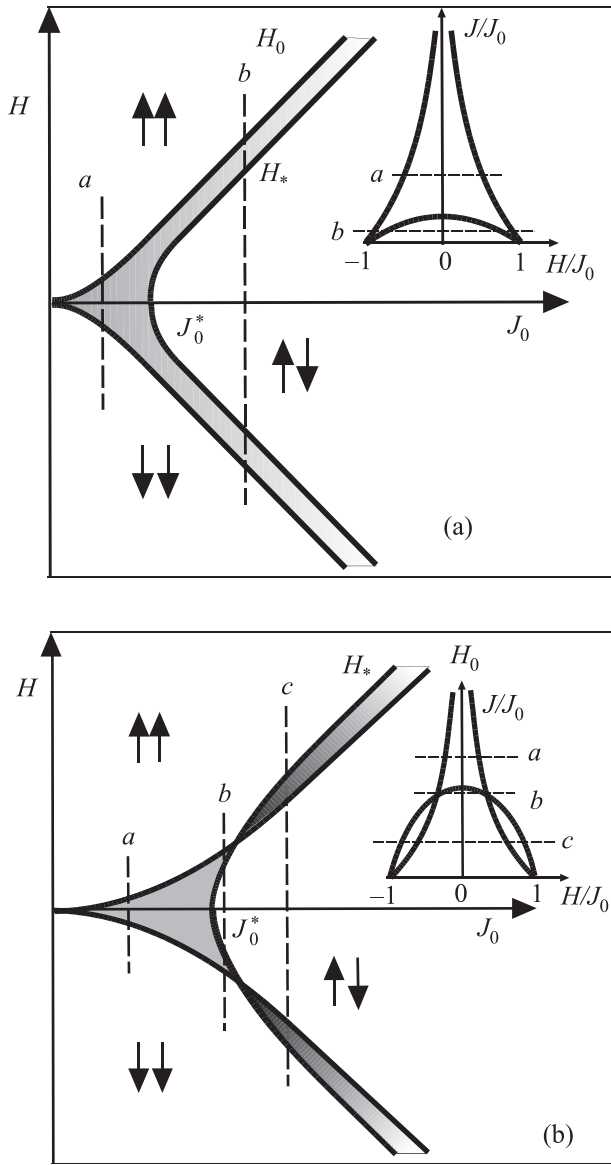


FIG. 4. Regions of collinear ($\uparrow\uparrow$ and $\downarrow\downarrow$), anti-collinear ($\uparrow\downarrow$), and canted (shaded in cross sections a and b), structures and hystereses (shaded in cross section c) at $L < L_0$. The insets show the dependence $J = J(H)$ for boundaries of different structures at a fixed value of the exchange interaction through the interface.

$$\varphi_A = A \operatorname{ch} \left(\sqrt{\frac{J_0 + H}{J}} \frac{x}{a} \right), \quad \psi_B = B \operatorname{ch} \left(\sqrt{\frac{J_0 - H}{J}} \frac{x - L}{a} \right). \quad (12)$$

The system in (11) is formally identical to the equations that describe linear parametric resonance in oscillation theory,

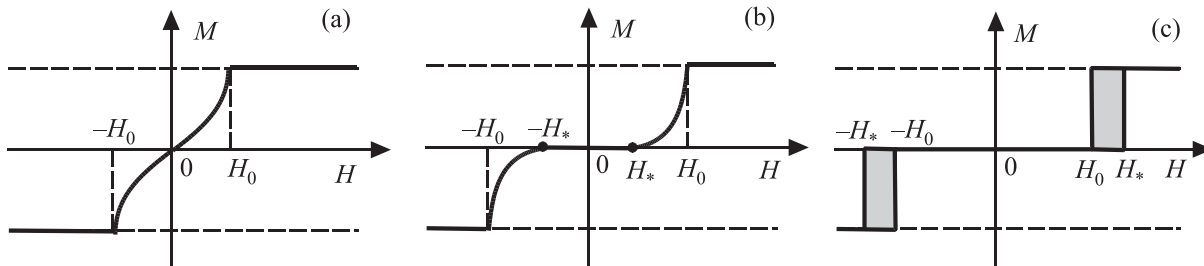


FIG. 5. Dependence of magnetization of the FM on the field at different values of the parameter for the exchange interaction through the interface, corresponding to lines a , b , and c , in Fig. 4.

whereas (12) corresponds to a symmetric single-frequency solution at the boundary of the stability region. In addition to the solution for (12), there exists an antisymmetric single-frequency solution, in which $\varphi_A = A \operatorname{sh}(\sqrt{(J_0 + H)/J} x/a)$, however, when it takes nonlinearity into account, it becomes unstable, and will not be used by us. Equation (11) are supplemented by boundary conditions (6), which are also linearized. As is with the previous case, the spatial derivatives are continuous: $\varphi'_A|_s = \varphi'_B|_s$, but the angle of magnetization rotation experiences a jump: $a\varphi'_A|_s = (\varphi_A + \psi_B)|_s$. These relations imply the dependence of the critical field H_* on the FM and interface parameters.

$$R_* \operatorname{th}(R_*) P_* \operatorname{th}(P_*) = \frac{L}{2a} [R_* \operatorname{th}(R_*) + P_* \operatorname{th}(P_*)], \quad (13)$$

where $R_* = S\sqrt{1 + h_*}$ and $P_* = S\sqrt{1 - h_*}$. This is shown in Fig. 4 in the form of $H_*(J, J_0, L)$ curves. The asymptote of the $H_*(J, J_0, L)$ function with the limit $H_* \rightarrow J_0$ looks like $H_* \approx J_0 - J(2a/L)$, and the minimum value of the exchange interaction J_0^* through the interface, at which the anti-collinear configuration and the “horizontal plateau” occur, is determined by equation $\sqrt{J_0^*/J} \operatorname{th}[(L/2a)\sqrt{J_0^*/J}] = 2$. For the limit $L \gg a$, this value is equal to $J_0^*/J \approx 4 + 16 \exp(-2L/a)$ and is close to 4, even at a high step density at the interface ($J_0^*/J \approx 4.005$ at $L = 4a$).

A comparison of the asymptotes at critical values $H_*(J \rightarrow 0)$ and $H_0(J \rightarrow 0)$, points to a different behavior of the magnetization curves given different values for the period of the interface structure. The typical value of this period is equal to $2L_0 = \pi^2 a$. At $L > L_0$, given changes in the external field, the magnetization changes monotonically in the $-H_0 < H < H_0$ interval at $J_0 < J_0^*$ (line a in Figs. 4(a) and 5(a)), or the “horizontal plateau” appears with $M = 0$ at $-H_* < H < H_*$, separated by sloped magnetization regions at $H_* < |H| < H_0$ intervals (line b in Figs. 4(a) and 5(b)). At a high density of atomic steps at the interface $L < L_0$ magnetization changes monotonically with the field at the $-H_0 < H < H_0$ interval at $J_0 < J_0^*$ (line a in Figs. 4(b) and 5(a)). In the $J_0^* < J_0$ region, there is a “horizontal plateau” separated by sloped regions with fields $H_* < |H| < H_0$ (line b in Figs. 4(b) and 5(b)). And given a large exchange interaction through the surface, the sloped regions of the field dependence of magnetization turn into hysteresis loops (line c Figs. 4(b) and 5(c)).

Therefore, in the proposed models, the hysteresis curves can exist even in the absence of single-ion anisotropy. This is related to the fact that there exists a symmetry of magnetic properties relative to the direction along the X axis, and the impact of the AFM subsystem acts as an effective magnetic anisotropy. However, while the width of the hysteresis loops

is usually determined by the value of the magnetic anisotropy, in the given case at $L < L_0$ and $J_0 \gg J$, the width of the hysteresis loops is equal to $\Delta H_h = J(2a/L)(L_0/L - 1)$, and the hysteresis loops have a strictly rectangular shape and do not contain any sloped regions. The insets in Fig. 4 show the dependence of the J/J_0 values on the external field H/J_0 , for the critical values of the field, at which the configuration of the distribution of FM magnetization changes. This is presented for the sake of comparison against research results involving the field dependence in the case of an ideal interface with a dual-layer FM. This question has been examined by us earlier in Ref. 8, where it was demonstrated that the indicated dependences in a simple dual-layer model have properties that match the results obtained in this study (Fig. 4 in Ref. 8).

In order to find the canted magnetic structures in the isotropic FM, it is necessary to solve the nonlinear equations (3), (4) with $\beta = 0$. These solutions are well-known:

$$\varphi_A = 2 \arcsin \left[k'_A / \operatorname{dn} \left(\sqrt{\frac{J_0 + H}{J}} \frac{x}{a}, k_A \right) \right], \quad (14)$$

$$\varphi_B = 2 \arcsin \left[k_B \operatorname{cn} \left(\sqrt{\frac{J_0 - H}{J}} \frac{x - L}{a}, k_B \right) / \operatorname{dn} \left(\sqrt{\frac{J_0 - H}{J}} \frac{x - L}{a}, k_B \right) \right], \quad (15)$$

where $\operatorname{cn}(r, k)$ and $\operatorname{dn}(r, k)$ are the Jacobi elliptic functions, k is the elliptic modulus, and the additional modulus $k' = \sqrt{1 - k^2}$. Solutions (14) and (15) turn into (12) at $k_A \rightarrow 1$ and $k_B \rightarrow 0$.

Substituting solutions (14) and (15) into formula (7) for the total FM magnetization, we get

$$M = M_m \left[\frac{k_A^2 \operatorname{cn}(R, k_A) \operatorname{sn}(R, k_A)}{R \operatorname{dn}(R, k_A)} - \frac{k_B^2 \operatorname{cn}(P, k_B) \operatorname{sn}(P, k_B)}{P \operatorname{dn}(P, k_B)} - \frac{E(\operatorname{am}(R, k_A))}{R} + \frac{E(\operatorname{am}(P, k_B))}{P} \right], \quad (16)$$

where $\operatorname{sn}(r, k)$ is the Jacobi elliptic sine, $E(r, k)$ is an incomplete elliptical integral of the second kind, defined as $E(u, q) = \int \sqrt{1 - q^2 \sin^2 u} du$, $R = S\sqrt{1 + h}$, $P = S\sqrt{1 - h}$, and $\operatorname{am}(r, k)$ is the elliptic amplitude. In this expression, the magnetic field is included in the parameters R and P , and in the elliptic moduli, k_A and k_B . The latter are determined by the boundary conditions (6):

$$\frac{k_A k'_A R \operatorname{sn}(R, k_A)}{\operatorname{dn}(R, k_A)} = \frac{k_B k'_B P \operatorname{sn}(P, k_B)}{\operatorname{dn}(P, k_B)}, \quad (17)$$

$$\begin{aligned} k_A k'_A \frac{R \operatorname{dn}(R, k_A) + \operatorname{cn}(R, k_A)}{\operatorname{dn}^2(R, k_A)} \\ + k_B k'_B \frac{P \operatorname{dn}(P, k_B) - \operatorname{cn}(P, k_B)}{\operatorname{dn}^2(P, k_B)} \\ = \frac{2k_A k'_A k_B'^2 \operatorname{cn}(R, k_A) - 2k_B k'_B k_A'^2 \operatorname{cn}(P, k_B)}{\operatorname{dn}^2(R, k_A) \operatorname{dn}^2(P, k_B)}. \end{aligned} \quad (18)$$

Equation (18) is simplified in the long-wave limit, when conditions (5) are met

$$\frac{k'_A}{\operatorname{dn}(R, k_A)} = \frac{k_B \operatorname{cn}(P, k_B)}{\operatorname{dn}(P, k_B)}, \quad (19)$$

and it's easy to find the elliptic moduli connection

$$k_B^2 = k_A'^2 \frac{2S^2 - R^2 \operatorname{dn}^2(R, k_A)}{(2S^2 - R^2) \operatorname{dn}^2(R, k_A)}. \quad (20)$$

The “horizontal plateau” at $M=0$ on the $M=M(H)$ curve is absent, but for certain parameter expressions, regions with a very small slope angle for this function, are possible (i.e., regions observed in the experiment). Equations (19) and (20) define the elliptic moduli $k_A(H)$, $k_B(H)$ as functions of the magnetic field, and after substituting them into expression (16) the field dependence of magnetization is found. In Fig. 6 this dependence is given for the parameters of the system: $J_0/J = 0.5$, and $L = 10a$.

The field dependence of magnetization at low values of the latter is easy to find using Eqs. (17) and (19). In the absence of a field, the values of the elliptic moduli $k_A = k_B = k_0$ are determined by the equation

$$\sqrt{2} k'_0 = \operatorname{dn}(S, k_0), \quad (21)$$

and change in the $k_0 = 1/\sqrt{2} - 1$ interval as parameter S grows from zero to infinity. The additional modulus k'_0 becomes anomalously small at values of $S \sim 2$. In small fields, the moduli k_A and k_B differ only slightly from k_0 , to the extent of the smallness of h . It is easy to show that these differences are determined by expression

$$\begin{aligned} k_{A,B} \approx k_0 \pm h \\ \times \frac{2k_0 [S + \operatorname{sn}(S, k_0) \operatorname{dn}(S, k_0)]}{2E[\operatorname{am}(S, k_0), k_0] - S \operatorname{dn}^2(S, k_0) - \operatorname{sn}(S, k_0) \operatorname{dn}(S, k_0)}, \end{aligned} \quad (22)$$

the substitution of which into formula (16) gives the slope of the magnetization curve in small fields, and describes the horizontal plateau on this dependence.

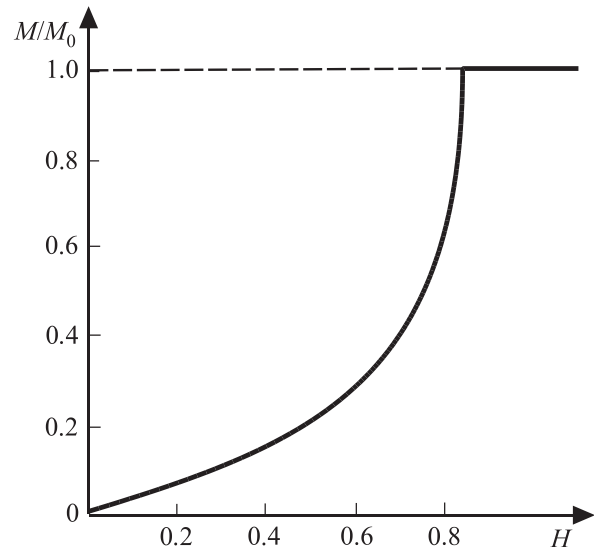


FIG. 6. Dependence of FM film magnetization on the external field, given $J_0/J = 0.5$ and $L = 10a$.

Formulas (21) and (22) define the relationships $k_0(S)$, $k_A(S)$ and $k_B(S)$, and consequently the dependence of magnetization on the field, and the parameters of the system. At small values of the parameter S , expression (22) is simplified to $k_0 = 1/\sqrt{2 - S^2}$ and $k_{A,B} = k_0(S) \pm h3\sqrt{2/S^2}$. The corresponding dependence of magnetization looks like this:

$$M \approx 12h/S^2, \quad S \ll 1. \quad (23)$$

In the opposite limit $S \gg 1$ (actually, at $S > 2$)

$$M = M_m \left(\frac{k_A^2 \operatorname{cn}(R, k_A) \operatorname{sn}(R, k_A)}{R \operatorname{dn}(R, k_A)} - \frac{k_B^2 \operatorname{cn}(P, k_B) \operatorname{sn}(P, k_B)}{P \operatorname{dn}(P, k_B)} - \frac{E[\operatorname{am}(R, k_A)]}{R} + \frac{E[\operatorname{am}(P, k_B)]}{P} \right), \quad (24)$$

and after a numerical solution of Eqs. (21) and (22), and substituting $k_{0,A,B}(h, S)$ into (24), we derive the dependence $M(H)$ shown in Fig. 6.

4. Inhomogeneous states of isotropic ferromagnetic film given an uncompensated interface ($b \neq L/2$)

We will examine the influence of an uncompensated interface, at which the areas with different directions of magnetization at the AFM boundary layer, are different sizes, i.e., ($b \neq L/2$), and the average magnetization of the subsurface AFM layer is other than zero (see Fig. 7).

In this case, the solutions for the distribution of magnetization in regions A and B still look like (9), (12), (14), and (15), but the boundary conditions (5) and (6) are formulated for $x = b \neq L/2$. (The average magnetization of the surface layer is equal to $M_0(2b - L)/L$, and the effective exchange constant through the interface is equal to $J_0/(2b - L)$.) In this case, for a positive direction of the external magnetic field ($H > 0$) Eq. (8) and solutions (9) are preserved, and the formula (10) that determines the critical fields, at which the non-collinear structures occur, is upgraded as follows:

$$P_0^+ \operatorname{tg} \left(P_0^+ \frac{2(L-b)}{L} \right) = R_0^+ \operatorname{th} \left(R_0^+ \frac{2b}{L} \right), \quad (25)$$

where $R_0^+ = (L/2a)\sqrt{(J_0 + |H_0^+|)/J}$ and $P_0^+ = (L/2a)\sqrt{(J_0 - |H_0^+|)/J}$.

With an opposite direction of the field ($H < 0$), formulas (8) for small deviations $\psi_{A,B} = \pi - \varphi_{A,B}$ from the state with $\varphi_{A,B} = \pi$, are transformed as follows:

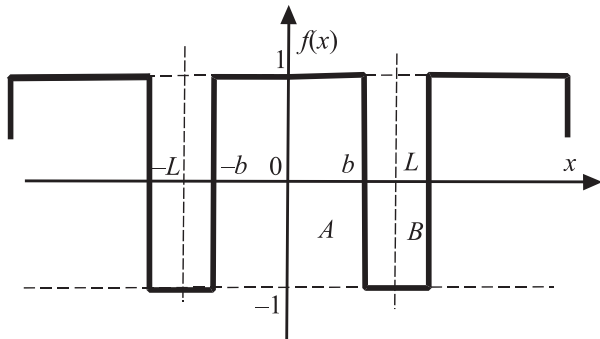


FIG. 7. Profile of the exchange interaction through the FM/AFM border, in the case of an uncompensated interface.

$$Ja^2\psi_A'' + (J_0 - |H|)\psi_A = 0, \quad Ja^2\psi_B'' + (J_0 - |H|)\psi_B = 0, \quad (26)$$

the solutions for which, replacing (9), look like

$$\psi_A = A \cos \left(\sqrt{\frac{J_0 - |H|}{J}} \frac{x}{a} \right), \quad \psi_B = B \operatorname{ch} \left(\sqrt{\frac{J_0 + |H|}{J}} \frac{x - L}{a} \right). \quad (27)$$

In this case, formula (25) also changes:

$$P_0^- \operatorname{tg} \left(P_0^- \frac{2b}{L} \right) = R_0^- \operatorname{th} \left(R_0^- \frac{2(L-b)}{L} \right), \quad (28)$$

where $R_0^- = (L/2a)\sqrt{(J_0 + |H_0^-|)/J}$ and $P_0^- = (L/2a)\sqrt{(J_0 - |H_0^-|)/J}$. The dependences $H_0^\pm = H_0^\pm(J_0)$ at fixed parameters J , L , and b , are shown in Fig. 9 in the form of H_0^\pm curves. Their asymptotes for large values of exchange interaction through the interface look like: $H_0^+ \approx J_0 - J[\pi a/2(L-b)]^2$ at $(J_0/J)[(L-b)/a]^2 \gg 1$ and $H_0^- \approx -J_0 + J(\pi a/2b)^2$ at $(J_0/J)(b/a)^2 \gg 1$. The asymptotes at small values of the exchange looks like: $H_0^\pm \approx J_0(1 - 2b/L)$. The derived dependences are shown in Fig. 9 as the $H_0^\pm(J_0)$ line.

As is the case with $b = L/2$, when the discreteness of the FM layer in the system is taken into account, a collinear structure can occur, manifesting in the form of a “horizontal plateau” on the $M(H)$ curve. In this phase, within the A region, the angle of magnetization rotation is equal to $\varphi = 0$, and in B regions it is $\varphi = \pi$. However, for $b \neq L/2$, the total FM magnetization in the horizontal plateau region is nonzero: the density of the magnetic moment is equal to $M = M_0(2b - L)/L$. For small deviations from this state, the solutions still look like (12), with boundary conditions at point $x = b \neq L/2$. In this case, formula (13) for the dependences of the critical fields on the J_0 parameter is upgraded, and looks like

$$R_*^\pm \operatorname{th} \left(R_*^\pm \frac{2b}{L} \right) P_*^\pm \operatorname{th} \left(P_*^\pm \frac{2(L-b)}{L} \right) = \frac{L}{2a} \left(R_*^\pm \operatorname{th} \left(R_*^\pm \frac{2b}{L} \right) + P_*^\pm \operatorname{th} \left(P_*^\pm \frac{2(L-b)}{L} \right) \right), \quad (29)$$

and the corresponding graphs are showing in Fig. 9 as the $H_*^\pm(J_0)$ line. The shape of the magnetization curves is essentially determined by the expressions for the parameters of the interface: L , b , and J_0 . The restructuring of field dependences can be assessed using the asymptotes of the critical fields at large values of exchange interaction through the interface ($J_0 \gg J$). These asymptotes look like: $H_0^+ \approx J_0 - J[\pi a/2(L-b)]^2$, $H_*^+ \approx J_0 - Ja/(L-b)$, $H_*^- \approx -J_0 + Ja/b$, $H_0^- \approx -J_0 + J(\pi a/2b)^2$. These expressions imply the existence of three different types of critical field relationships. They are shown in Figs. 9(a)–9(c), and they correspond to fields a , b , and c in Fig. 8.

In Fig. 9, lines a , b , c , d , and, e stand for values of the J_0 parameter, at which the field dependences of FM magnetization are markedly different in character. They are shown in Fig. 10.

5. Inhomogeneous states of anisotropic ferromagnetic film

Above, we have neglected the influence of the weak anisotropy in the easy plane, on the field dependence of the FM

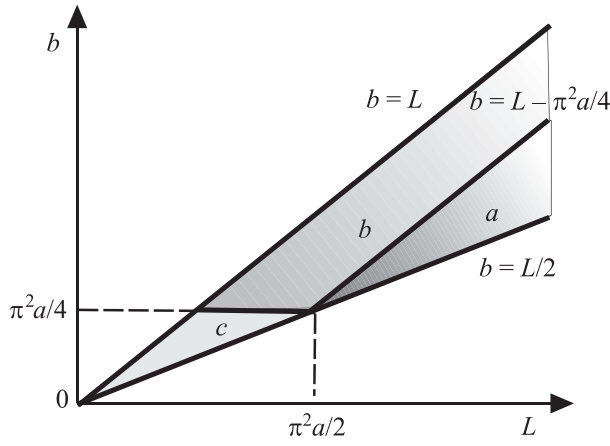


FIG. 8. Regions of existence for the solutions of different types of dependences, on the degree of interface roughness (expressions for parameters L and b).

film. However, taking it into account is essential, since it determines the hysteresis dependences of magnetization. In the case of an ideal interface, this influence was examined by is in Refs. 7 and 8. The magnetic anisotropy is not included in boundary conditions (5) and (6), but only in Eqs. (3) and (4).

We will return to the initial Eqs. (3) and (4), taking into account the last terms thereof, and we will find the critical values of the magnetic field, at which the bifurcation of the solutions into collinear and anti-collinear homogeneous states occurs. The knowledge of these critical fields provides for the possibility of giving a quality description of how the field dependences are transformed with the inclusion of anisotropy. The boundary of the collinear state stability $H = H_0^+$ with $\varphi_1 = \varphi_2 = 0$ is determined by the linearized Eqs. (3) and (4) in close proximity to this state, and leads to Eq. (8), in which the magnetic field varies by the value β : $H \rightarrow H + \beta$. In this case, solutions (9) for φ_A and φ_B , expressions (10) (for the compensated interface), and (25) (for the uncompensated interface), all retain their form with the substitution of $H \rightarrow H + \beta$. Consequently, there occurs a shift in the critical field $H_0^+ \rightarrow H_0^+ - \beta$. The boundary of the collinear state stability $H = H_0^-$ with $\varphi_1 = \varphi_2 = \pi$, is determined by Eq. (31), in which $|H| \rightarrow |H| + \beta$, solutions (27), and expression (28), all retain their form after this substitution. Thus, the critical field changes as follows: $H_0^- \rightarrow H_0^- + \beta$.

For the anti-collinear structure with $\varphi_1 = 0$, $\varphi_2 = \pi$, the existence boundaries are determined by Eq. (11), in which the parameter J_0 is substituted by the value $J_0 + \beta$. Respectively, such a substitution must be done in solution (12) and expressions (13), for the compensated interface, and (29) for the uncompensated interface. Therefore, for a fixed value of the field H_* , the corresponding critical value of the exchange through the interface is $J_0 \rightarrow J_0 - \beta$. Consequently, in Figs. 4 and 9, the dependences $H_0^+(J_0)$ and $H_0^-(J_0)$ shift to lower fields, by β , and dependences $H_*^+(J_0)$ and $H_*^-(J_0)$ to lower values of J_0 by the same amount, β .

We will first examine the instance of the compensated interface with $b = L/2$. We will limit ourselves to the long-wave approximation with boundary conditions (5), which give the expressions (10) with the indicated substitution of the field value. At such boundary conditions, the anti-collinear structure is absent, and regions of collinear distribution of

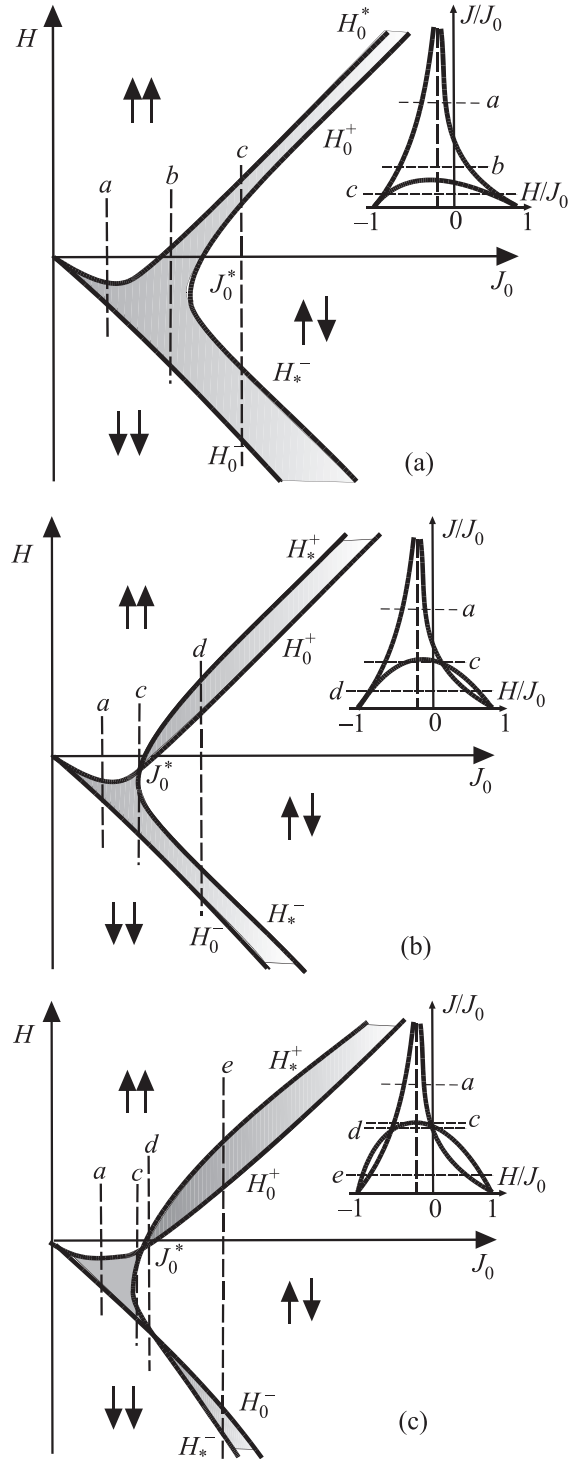


FIG. 9. Regions of collinear ($\uparrow\uparrow$ and $\downarrow\downarrow$), anti-collinear ($\uparrow\downarrow$), and canted (shaded) structures and hystereses (shaded) at $L/2 < b < L - \pi^2 a/4$ (a), $\pi^2 a/4 < L - \pi^2 a/4 < b < L$ (b), $L/2 < b < L$, $\pi^2 a/4$ (c). The insets show the dependence $J = J(H)$ for boundaries of different structures at a fixed value of the exchange interaction through the interface.

magnetization ($\uparrow\uparrow$ and $\downarrow\downarrow$) in the parameter plane are divided by a canted phase region. In this case, the graph in Fig. 4(a) is updated by using the following method (see Fig. 11).

In Fig. 11, the thick lines H_0^* indicate the boundaries of the region in which collinear phases $H_0 - \beta$ and $-H_0 + \beta$ exist. Thin boundary lines of the shaded hysteresis regions $\pm \tilde{H}$ correspond to states in which $dM/dH = 0$. These boundaries cannot be found from the solutions of the linearized solution, and it is necessary to examine the initial nonlinear

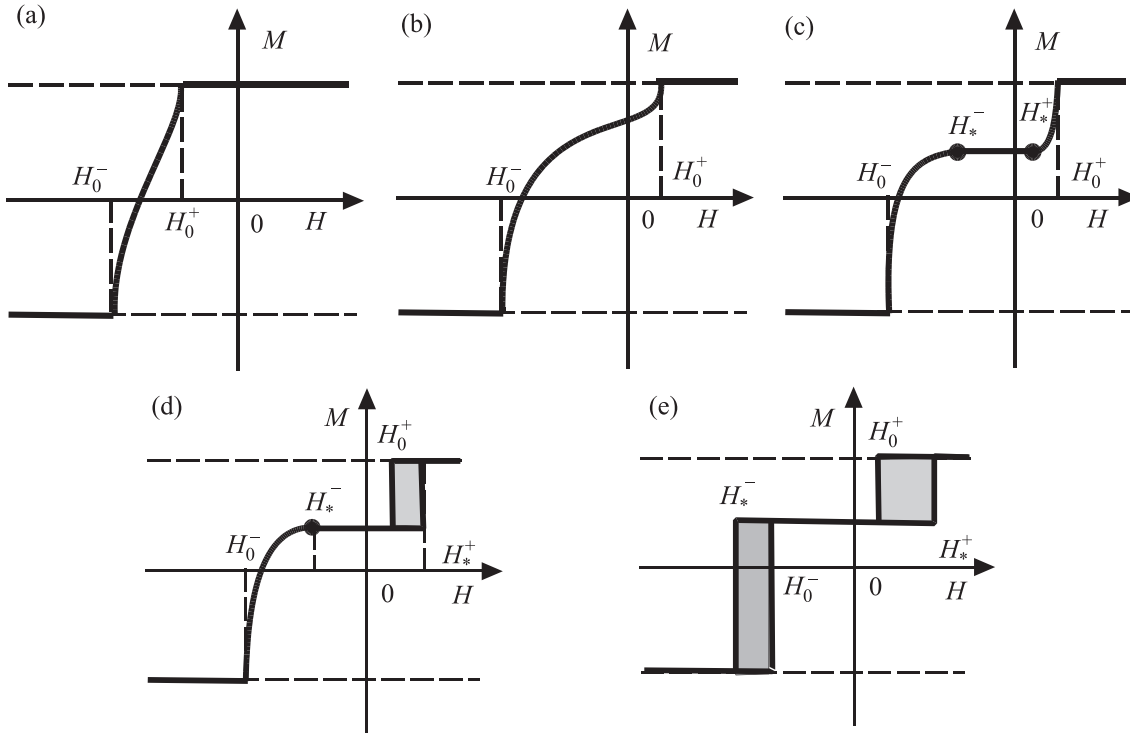


FIG. 10. Dependences of FM magnetization on the field, at different values of the parameter of the exchange interaction through the interface, corresponding to lines *a, b, c, d*, and *e* in Fig. 9.

equations, which is fairly difficult. Therefore below, this problem is examined numerically within the framework of a discrete approach. However, it can be said that the width of the hysteresis regions has the order of magnitude of the magnetic anisotropy, β . In Fig. 11 lines *a, b, c, d*, and *e*, denote the values of the parameter J_0 , at which the field dependences of FM magnetization are different. They are shown in Fig. 12.

The critical value of the exchange interaction through the interface J_0^* , at which the “split” of the hysteresis loops into two separate loops occurs, corresponding to line *b* in Fig. 11, is determined by the condition $H_0(J_0^*) - \beta = -H_0(J_0^*) + \beta$.

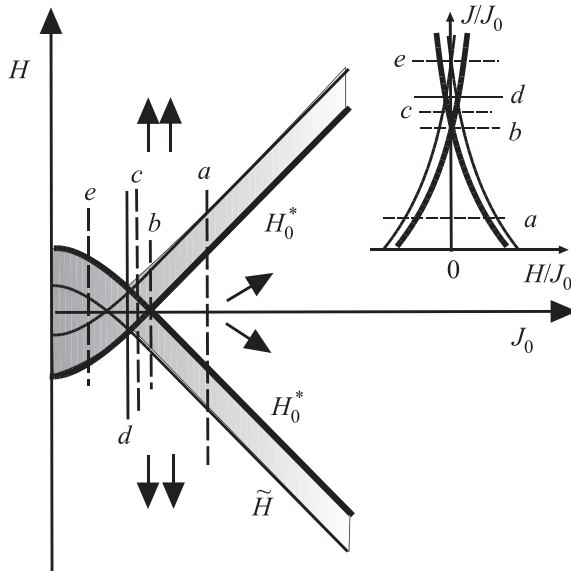


FIG. 11. Regions of collinear ($\uparrow\uparrow$ and $\downarrow\downarrow$), and canted structures, and also regions of hysteresis (shaded).

In this case, the expression (10) reduces to the following equation for J_0^* :

$$\sqrt{J_0^* - \beta} \operatorname{tg} \left(\frac{L}{2a} \sqrt{\frac{J_0^* - \beta}{J}} \right) = \sqrt{J_0^* + \beta} \operatorname{tg} \left(\frac{L}{2a} \sqrt{\frac{J_0^* + \beta}{J}} \right). \quad (30)$$

Its solution is easy to find within the limits of the weak and strong roughness of the interface. At fixed parameters J and β of the FM film, within the limit of weak roughness $L/a \gg \sqrt{J/\beta}$, we have $J_0^* \approx \beta$, and at a strong roughness of the boundary $L/a \ll \sqrt{J/\beta}$, the critical value of the exchange through the interface is equal to $J_0^* \approx (a/L)\sqrt{12J\beta}$.

The case of the uncompensated boundary of the FM/AFM partition is more difficult to examine. Therefore, we will limit ourselves to a qualitative assessment of this system, and will use more accurate discrete boundary conditions (6) at points $x = b \neq L/2$. In this case, the linearized Eqs. (3) and (4), and linearized boundary conditions (6) give, in addition to the boundary field values H_0^+ and H_0^- , additional “fiducial” points H_*^+ and H_*^- , allowing us to restore the qualitative form of the dependences of magnetization on the external field at different values of parameters J_0 , L , and b . At large values for the parameter J_0 , the asymptotes of the critical field values look like

$$H_0^+ = J_0 - J[\pi a/2(L-b)]^2 - \beta, \quad H_0^- = -J_0 + J(\pi a/2b)^2 + \beta, \\ H_*^+ = J_0 - J[a/(L-b)] - \beta, \quad H_*^- = -J_0 + J[a/b] + \beta.$$

We can see from these formulas, that at different degrees of roughness, the interface boundary regions

$$L/2 < b < L - \pi^2 a/4, \quad \pi^2 a/4 < L - \pi^2 a/4 < b < L, \\ L/2 < b < L, \quad \pi^2 a/4$$

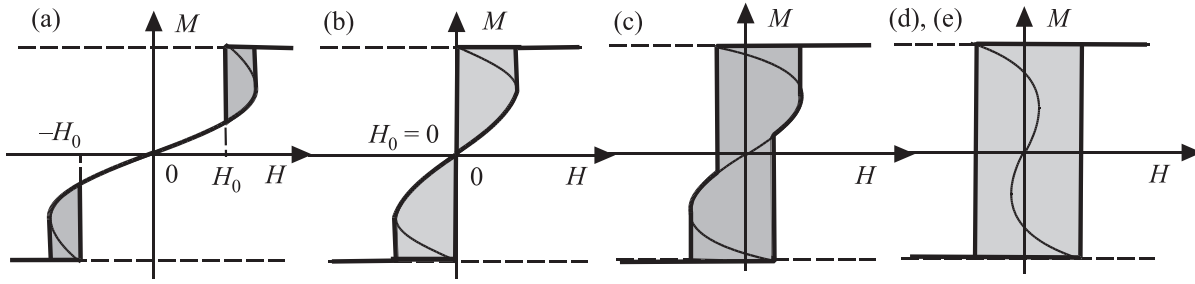


FIG. 12. Dependences of FM magnetization on the field, at different values of the parameter of the exchange interaction through the interface, corresponding to lines *a, b, c, d*, and *e* in Fig. 11.

with different $M(H)$ dependences, remain the same in the absence of anisotropy. Since in the absence of anisotropy for field values $H = H_0^\pm$, the derivative $dH/dM = \infty$, whereas for $H = H_*$ the derivative is zero, then when magnetic anisotropy is taken into account, the hysteresis loops occur only in proximity to the critical values $H = H_0^\pm$. Taking into account the above-mentioned shifts in the dependence lines of the critical fields due to the J_0 parameter, we get the graphs pictured in Fig. 12. In these diagrams, dark shaded areas are the hysteresis regions, and the light shading represents regions of anti-collinear FM structure.

Field hysteresis dependences of magnetization, having a sufficiently different character and corresponding to the values of exchange interaction through the interface, are marked in Fig. 13 by lines *a, b, c, d*, and *f*, shown in Fig. 14.

Therefore, the field dependences of magnetization obtained within the framework of the simple proposed models, are shown in Figs. 5, 10, 12, and 14, and describe the diversity of experimentally-observed field dependences of layered ferro/antiferromagnetic systems.

6. The effect of discreteness of the stepped FM/AFM border, on the field dependence of the system

The above-examined ferro/antiferromagnet system, with periodically arranged atomic steps along the interface, can also be examined within the framework of a discrete model.^{5,7,8} In our previous studies, it is demonstrated that the hysteresis loops occurring in such systems, may take a form that is qualitatively similar to the results of a continuum model,^{7,12} in addition, magnetization curves may have properties that are absent in the continuum model.⁷

Equations for the arrangement of magnetization in regions *A* and *B*, corresponding to Eqs. (3) and (4), will look like

$$(H + J_0) \sin \varphi_n + J \sin (\varphi_n - \varphi_{n+1}) + J \sin (\varphi_n - \varphi_{n-1}) + \beta \sin \varphi_n \cos \varphi_n = 0 (A), \quad (31)$$

$$(H - J_0) \sin \varphi_n + J \sin (\varphi_n - \varphi_{n+1}) + J \sin (\varphi_n - \varphi_{n-1}) + \beta \sin \varphi_n \cos \varphi_n = 0 (B). \quad (32)$$

The structure of the interface, as before, is assumed to be periodic, and the atomic cell of the period with N nodes can contain one region *A* and *B* each, as well as several such regions of different sizes. This system, in addition to canted solutions, allows for the existence of collinear $\varphi_n^A = \varphi_n^B = 0$ and $\varphi_n^A = \varphi_n^B = \pi$, and anti-collinear $\varphi_n^A = 0, \varphi_n^B = \pi$ configurations.

As is the case with the continuum model, first we will find the critical values of the field, at which the collinear and anti-collinear structures lose stability, in the case of an isotropic ferromagnetic film with $\beta = 0$, coming into contact with an AFM, with atomic step defects along the interface. Thus

$$H_0^+ = -2J + \sqrt{4J^2 + J_0^2}, \quad H_0^- = 2J - \sqrt{4J^2 + J_0^2}.$$

Exact analytical expressions for the dependence of magnetization on the external magnetic field, in a discrete model, are easy to find in the absence of magnetic anisotropy in the easy plane, for system size $N = 2$, when regions *A* and *B* contain only one atom each, and the structure of the boundary AFM layer looks like $\dots \uparrow \downarrow \uparrow \downarrow \uparrow \downarrow$. This simplest model of the period structure, corresponds to the ideal compensated

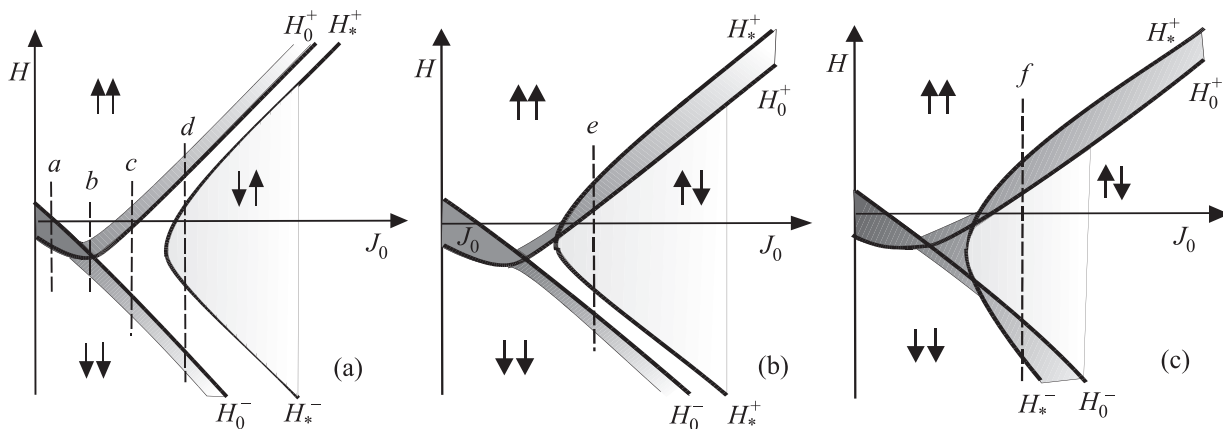


FIG. 13. Regions of collinear ($\uparrow\uparrow$ and $\downarrow\downarrow$), anti-collinear ($\uparrow\downarrow$) (light shading), canted structures and hystereses (dark shading), at $L/2 < b < L - \pi^2 a/4$ (a), $\pi^2 a/4, L - \pi^2 a/4 < b < L$ (b), $L/2 < b < L, \pi^2 a/4$ (c).

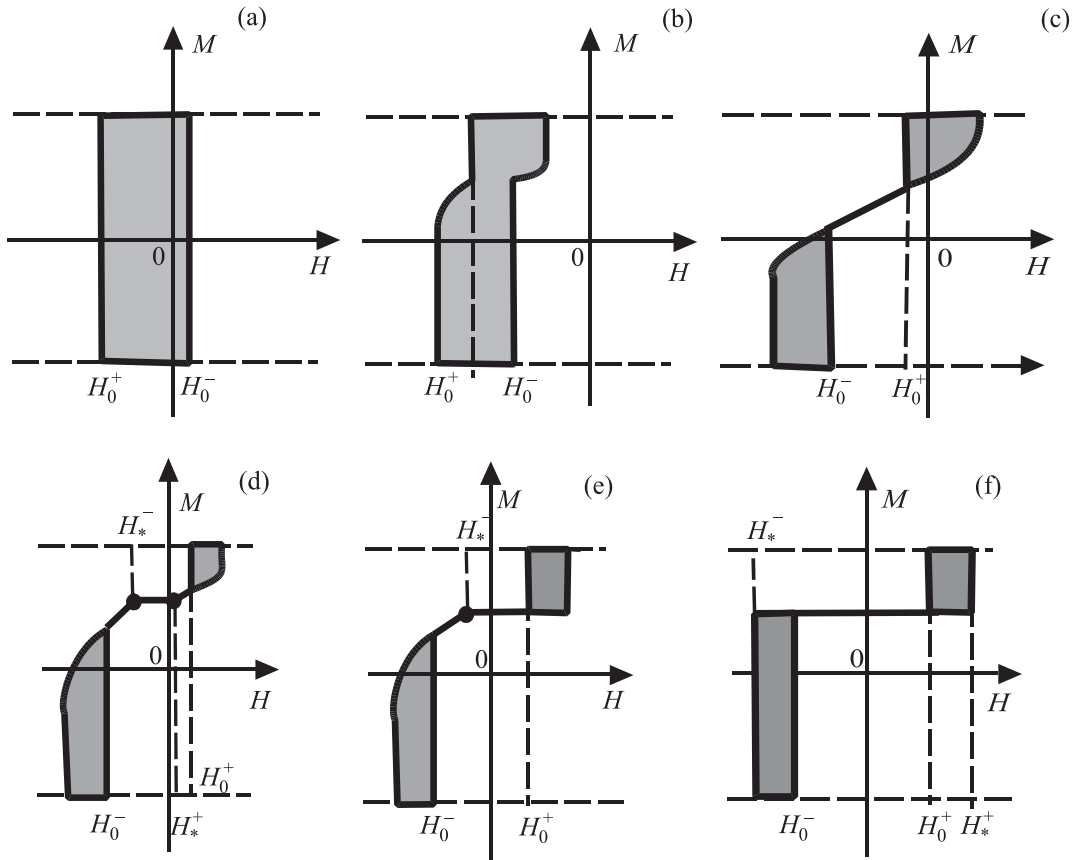


FIG. 14. Dependences of FM magnetization on the field, at different values of the parameter of the exchange interaction through the interface, corresponding to lines *a, b, c, d, e*, and *f* in Fig. 13.

boundary between the FM and AFM, with checkerboard ordering of the magnetic moments. In this case, the magnetization curves $M(H)$ were derived numerically, using a relaxation algorithm, and the energy minimum was found from the numerical solution of the system of differential equations $\partial\varphi_i/\partial t = \partial E/\partial\varphi_i$.⁸ In addition, the dependences $H_0^\pm(J_0)$ and $H_*^\pm(J_0)$ shown in Fig. 15, bear a qualitative resemblance as the dependences derived earlier within the framework of the continuum model (see Fig. 4(a)).

The dependences of the magnetization on the external magnetic field in this case, are shown in Fig. 16(a). Here, the

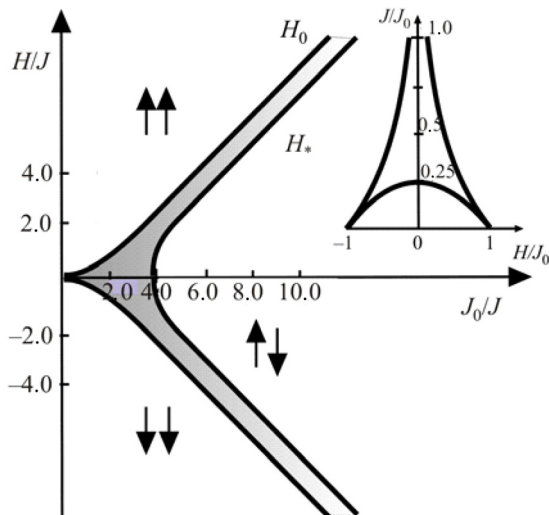


FIG. 15. Regions of collinear ($\uparrow\uparrow$ and $\downarrow\downarrow$), and canted structures.

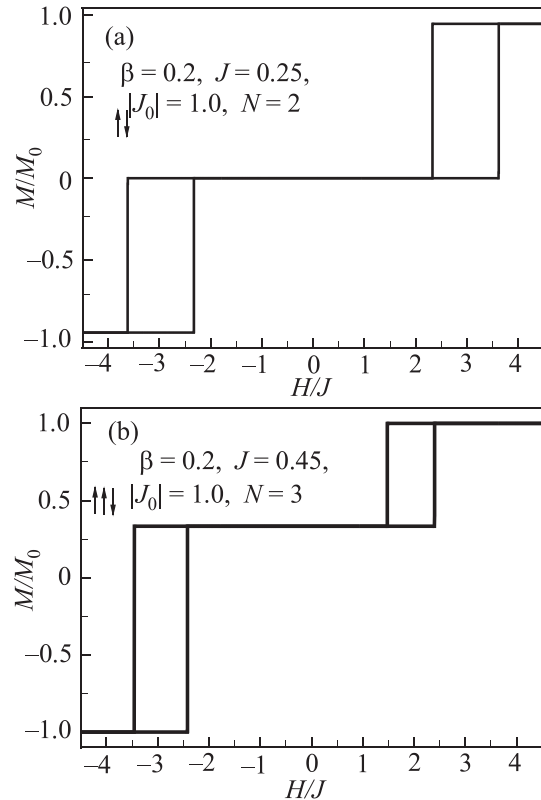


FIG. 16. Dependence of the magnetization, M/M_0 on the external magnetic field H/J for a system of periodic steps (a) and steps with double periodicity (b) at the FM/AFM border. The values of the system parameters are shown in the figure.

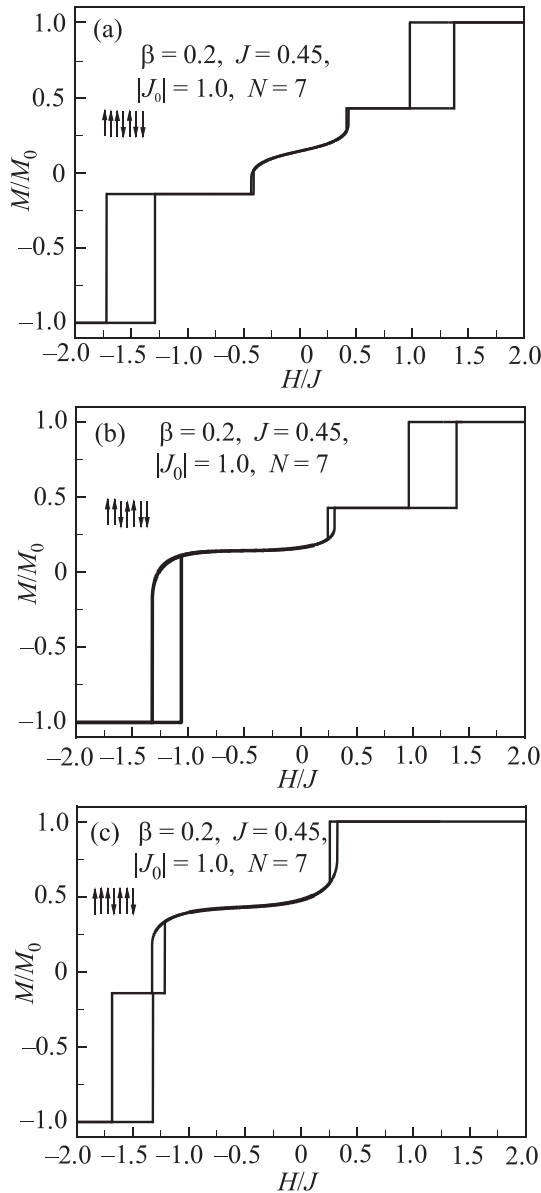


FIG. 17. Dependence of magnetization on the external magnetic field, for a system of steps at the FM/AFM border, with the period $N = 7$ and varying magnetic structure. The values of the system parameters and the period structure are shown in the figure.

shift of the magnetization curve is absent, and the curve is symmetrical relative to $H = 0$, but two hysteresis loops are observed, divided by a horizontal plateau with $M = 0$. These magnetization dependences were experimentally observed, for example, in Refs. 15 and 16. The shifted hysteresis loops, accompanied by a shift in the horizontal plateau with $M \neq 0$, occur in systems with atomic steps of double periodicity at the FM/AFM border, when the size of domains A and B is different (see Figs. 7 and 11 for continuum consideration). The numerical calculation of the corresponding simple discrete system with $N = 3$ similar to $\dots \uparrow \uparrow \uparrow \downarrow \uparrow \downarrow \uparrow \downarrow \dots$ gives the dependence $M(H)$, shown in Fig. 16(b), and one that qualitatively agrees with the result of the calculation of the continuum model (see Fig. 11).

Above, we examined interfaces with periodic surface structures, in which the period contained only one A and B domain. Real atomic step alternating-sign defects occur at random along the interface. In the first approximation, this

randomness can be modeled by a periodic system of defects with a more complex period structure. We numerically examined a system with $N = 7$, with identical magnetic parameters J, J_0 , and β , but a different arrangement of defects (steps) within the cell: $\dots |\uparrow \uparrow \uparrow \downarrow \uparrow \downarrow \uparrow \downarrow \uparrow \downarrow \uparrow \downarrow \dots$ (a) where the domains $A_3B_1A_1B_2$ alternate and $\dots |\uparrow \uparrow \uparrow \downarrow \uparrow \downarrow \uparrow \downarrow \uparrow \downarrow \uparrow \downarrow \dots$ (b) with domains $A_3B_1A_2B_1$. In cases (a) and (b) the average value of the exchange interaction through the interface is identical and equal to $\langle J_0 \rangle = 1/7$. However the different arrangement of the atomic steps within the period, leads to changes in the magnetization curves, even though the general structure of the field dependence stays the same (see Figs. 17(a) and 17(b)). Fig. 17(c) shows the field dependence of magnetization for a system with the same period $N = 7$, but another value of the average exchange interaction through the interface: $\langle J_0 \rangle = 3/7$. We see a large exchange bias and an increase in magnetization, corresponding to the ledge along the dependence $M(H)$. The figures show that the curves of magnetization can differ sufficiently, however there is a general structure to these dependences: the existence of two (or sometimes three) hysteresis loops, divided by a canted phase region with a unique dependence $M(H)$. With a stochastic distribution of surface defects, there must be an averaging of the obtained dependences, with the preservation of the main motive, that given certain values of the system parameters, there is a split of the hysteresis loop, and the occurrence of sloped regions of magnetization in-between the division.

7. Conclusion

In this paper, a simple model of a rough interface between the AFM and FM film, describing the periodic and doubly periodic stepwise structure of the interface with a long-wave limit, and a more complex periodic sequence of steps on the surface, via a discrete approach, the FM film magnetization field dependences are obtained for different parameters of the film (exchange interaction and magnetic anisotropy) and the interface (exchange interaction through the interface and the period of its step structure). It is demonstrated, that the obtained analytical and numerical results qualitatively describe the variety of known experimental data.

^aEmail: pankratova@ilt.kharkov.ua

¹J. Nogues and I. K. Schuller, *J. Magn. Magn. Mater.* **192**, 203 (1999).

²A. E. Berkowitz and K. Takano, *J. Magn. Magn. Mater.* **200**, 552 (1999).

³W. H. Meiklejohn and C. P. Bean, *Phys. Rev.* **102**, 1413 (1956).

⁴M. Kiwi, *J. Magn. Magn. Mater.* **234**, 584 (2001).

⁵A. G. Grechnev, A. S. Kovalev, and M. L. Pankratova, *Fiz. Nizk. Temp.* **35**, 603 (2009) [*Low Temp. Phys.* **35**, 476 (2009)].

⁶A. G. Grechnev, A. S. Kovalev, and M. L. Pankratova, *Fiz. Nizk. Temp.* **35**, 670 (2009) [*Low Temp. Phys.* **35**, 526 (2009)].

⁷A. G. Grechnev, A. S. Kovalev, and M. L. Pankratova, *Fiz. Nizk. Temp.* **39**, 1361 (2013) [*Low Temp. Phys.* **39**, 1060 (2013)].

⁸A. G. Grechnev, A. S. Kovalev, and M. L. Pankratova, *Fiz. Nizk. Temp.* **38**, 1184 (2012) [*Low Temp. Phys.* **38**, 937 (2012)].

⁹D. N. Merenkov, A. N. Bludov, S. L. Gnatchenko, M. Baran, R. Szymczak, and V. A. Novosad, *Fiz. Nizk. Temp.* **33**, 1260 (2007) [*Low Temp. Phys.* **33**, 957 (2007)].

¹⁰S. L. Gnatchenko, D. N. Merenkov, A. N. Bludov, V. V. Pishko, Yu. A. Shakhayeva, M. Baran, R. Szymczak, and V. A. Novosad, *J. Magn. Magn. Mater.* **307**, 263 (2006).

¹¹L. S. Uspenskaya, *Phys. Status Solidi* **52**, 2274 (2010).

¹²A. P. Malozemoff, *Phys. Rev. B* **35**, 3679 (1987).

- ¹³R. Coehoorn, J. T. Kohlhepp, R. M. Jungblut, A. Reinders, and M. J. Dekker, [Physica B](#) **319**, 141 (2002).
- ¹⁴A. S. Kovalev and M. L. Pankratova, *Fiz. Nizk. Temp.* **37**, 1085 (2011) [*Low Temp. Phys.* **33**, 866 (2011)].
- ¹⁵C. L. Chien, V. S. Gornakov, V. I. Nikitenko, A. J. Shapiro, and R. D. Shull, *Phys. Rev. B* **68**, 014418 (2003).
- ¹⁶N. J. Gokemeijer, J. W. Cai, and C. L. Chien, [Phys. Rev. B](#) **60**, 3033 (1999).
- ¹⁷A. Kovalev and M. Pankratova, [Superlattices Microstruct.](#) **73**, 275 (2014).

Translated by A. Bronskaya